MolecularMedicine

A Coding Variant of *ANO10*, Affecting Volume Regulation of Macrophages, Is Associated with *Borrelia* Seropositivity

Christian Hammer,[1] Podchanart Wanitchakool,[2] Lalida Sirianant,[2] Sergi Papiol,[1] Mathieu Monnheimer,[1] Diana Faria,[2] Jiraporn Ousingsawat,[2] Natalie Schramek,[3] Corinna Schmitt,[4] Gabriele Margos,[5] Angelika Michel,[6] Peter Kraiczy,[7] Michael Pawlita,[6] Rainer Schreiber,[2] Thomas F Schulz,[4] Volker Fingerle,[5] Hayrettin Tumani,[3] Hannelore Ehrenreich,[1,8] and Karl Kunzelmann[2*]*

[1]Clinical Neuroscience, Max Planck Institute of Experimental Medicine, Göttingen, Germany; [2]Institut für Physiologie, Universität Regensburg, Regensburg, Germany; [3]Department of Neurology, University of Ulm, Ulm, Germany; [4]Institute of Virology, Hannover Medical School, Hannover, Germany; [5]National Reference Center for Borrelia, Bavarian Health and Food Safety Authority, Oberschleissheim, Germany; [6]Division of Genome Modifications and Carcinogenesis, Infections and Cancer Program, German Cancer Research Center, Heidelberg, Germany; [7]Institute of Medical Microbiology and Infection Control, University Hospital of Frankfurt am Main, Frankfurt/Main, Germany; and [8]DFG Research Center for Nanoscale Microscopy and Molecular Physiology of the Brain (CNMPB), Göttingen, Germany

In a first genome-wide association study (GWAS) approach to anti-*Borrelia* seropositivity, we identified two significant single nucleotide polymorphisms (SNPs) (rs17850869, $P = 4.17E-09$; rs41289586, $P = 7.18E-08$). Both markers, located on chromosomes 16 and 3, respectively, are within or close to genes previously connected to spinocerebellar ataxia. The risk SNP rs41289586 represents a missense variant (R263H) of anoctamin 10 (ANO10), a member of a protein family encoding Cl^- channels and phospholipid scramblases. ANO10 augments volume-regulated Cl^- currents (I_{Hypo}) in *Xenopus* oocytes, HEK293 cells, lymphocytes and macrophages and controls volume regulation by enhancing regulatory volume decrease (RVD). ANO10 supports migration of macrophages and phagocytosis of spirochetes. The R263H variant is inhibitory on I_{Hypo}, RVD and intracellular Ca^{2+} signals, which may delay spirochete clearance, thereby sensitizing adaptive immunity. Our data demonstrate for the first time that ANO10 has a central role in innate immune defense against *Borrelia* infection.

Online address: http://www.molmed.org
doi: 10.2119/molmed.2014.00219

INTRODUCTION

Lyme borreliosis, caused by bacteria mainly transmitted by ticks of the genus *Ixodes*, is the most common tick-borne disease in Europe and the United States (1). It involves many organs, predominantly skin, musculoskeletal system, heart and nervous system (2). Central nervous system manifestations can imitate a broad range of neuropsychiatric syndromes (3), in rare cases even be indistinguishable from acute schizophrenia (4). Borreliosis is caused by a variety of species of *Borrelia burgdorferi sensu lato* complex, some of which show distinct differences in their pathogenic properties in the human host (5). *Borrelia* species have a highly complex genomic structure and genetic variation may account for a large proportion of the variability of pathogenicity (6). However, pathogens are not only depending on their own fitness for a successful establishment of infection, but also on the genetic makeup of their hosts. The recent years have produced a wealth of studies elucidating the important role of human genomic variation in host defense mechanisms, both for viral and bacterial infections (7). Given the immense phenotypic variation of *Borrelia* disease symptoms, it is likely that part of the variation is due to differences in human immune response, originating in genomic variation. We therefore set out to (i) identify host genomic variants mediating differential susceptibility to *Borrelia* infection/seropositivity

**HE and KK are joint senior authors.*

Address correspondence to *Hannelore Ehrenreich, Clinical Neuroscience, Max Planck Institute of Experimental Medicine, 37075 Göttingen, Germany. Phone: +49-551-3899-615; Fax: +49-551-3899-670; E-mail: ehrenreich@em.mpg.de; or Karl Kunzelmann, Department of Physiology, University of Regensburg, 93053 Regensburg, Germany. Phone: +49-941-943-4302; Fax: +49-941-943-4315; E-mail: Karl.Kunzelmann@ur.de.*

Submitted November 3, 2014; Accepted for publication February 23, 2015; Published Online (www.molmed.org) February 23, 2015.

by means of a genome-wide association study (GWAS) and to (ii) uncover a possible contribution of *Borrelia* seropositivity to core phenotypes of neuropsychiatric disorders. For advancing these objectives, we employed the Göttingen Research Association for Schizophrenia (GRAS) sample (8,9) comprised of 1,271 healthy blood donors and 1,224 patients suffering from neuropsychiatric disease.

MATERIALS AND METHODS

Participants

All subject data were collected in accordance with ethical guidelines and the Helsinki Declaration (10). Regarding the discovery sample (total of N = 2,495), subject selection was unbiased, that is, sera collection was concluded before specific serological analysis was planned: Schizophrenic patients (N = 1,076) were recruited between 2005 and 2011 at 23 German sites for the Göttingen Research Association for Schizophrenia (GRAS) data collection. Patients fulfilling *Diagnostic and Statistical Manual of Mental Disorders*, 4th edition (DSM-IV) (11) criteria for schizophrenia (81.4%) or schizoaffective disorder (18.6%) were included regardless of disease stage (8,12). Healthy GRAS controls were anonymized blood donors (N = 1,271; Transfusion Medicine, Göttingen, Department of Transfusion Medicine, University Medicine of Göttingen). Health was ensured by predonation screening (questionnaires, interviews, hemoglobin, blood pressure, pulse, temperature). Patients with affective disorders (N = 146) also were included (ongoing GRAS extension). Exploration sample (N = 100): In Ulm, a total of 257 patients with documented history of *Borrelia* infection were contacted in written form, resulting in 100 individuals interested in participating. The study included (a) a comprehensive history on tick bite and borreliosis-specific symptoms, (b) a neurological examination with special emphasis on cerebellar signs and (c) drawing of blood for genetic and serological analyses. Patients were classified in three subgroups based on clinical and serological findings (i) neuroborreliosis, (ii) systemic borreliosis or (iii) laboratory-based borreliosis without typical clinical signs and symptoms.

Phenotypical Analyses

Of all schizophrenic (GRAS) patients, extensive phenotypical characterization was conducted as referenced previously (8,12). Age of onset, age at first psychotic episode, positive and negative syndrome scale (PANSS) scores, chlorpromazine equivalents (CPZ), neurological symptoms (Cambridge Neurological Inventory [CNI]) including fine motor skills (MacQuarrie dotting/tapping), current cognitive functioning (composite score comprising reasoning, executive function, verbal learning and memory), global assessment of functioning (GAF), Parkinsonism, hard neurological signs, motor coordination, sensory integration and gait were employed as disease characteristics. Moreover, patient self-rating was performed using the Brief Symptom Inventory (BSI) (13). The Ulm borreliosis patients had a comprehensive clinical neurological, serological, and in 81 of 100 patients, also cerebrospinal fluid (CSF) examination. CSF diagnostics included leukocyte and differential cell count; nephelometric determination of total protein; CSF:serum ratios for albumin, IgG, IgA, and IgM; enzyme-linked immunosorbent assay (ELISA) for *Borrelia*-specific antibodies; and oligoclonal IgG analysis in CSF and serum by immunoelectrophoresis.

Serological Analyses

The presence of antibodies against *Borrelia* was first determined using Enzygnost Lyme link VlsE/IgG, a quantitative immunoenzymatic method based on a mix of native *Borrelia* antigens from *B. afzelii* strain PKo and recombinant VlsE obtained from three genospecies pathogenic to humans (*B. Burgdorferi sensu stricto*, *B. garinii*, *B. afzelii*) (Siemens Healthcare Diagnostics GmbH, Eschborn, Germany). Assays were processed automatically on BEP III (Siemens Healthcare Diagnostics GmbH) and interpreted (manufacturer's instructions) as positive, negative or borderline. Positive and borderline samples were reanalyzed using the Euroline Borrelia-RN-AT immunoblot (Euroimmun, Lübeck, Germany). Only the confirmed were defined seropositive for statistical analysis and contrasted against all others. Titer levels, when mentioned in the manuscript, refer to the enzyme-linked immunosorbent assay (ELISA) results. To test for specificity of association signals, the following immunoenzymatic assays were conducted: Novagnost Chlamydia pneumoniae IgG; Novagnost Chlamydia trachomatis IgG; Novagnost Mycoplasma pneumoniae IgG; and Enzygnost Anti-Helicobacter pylori/IgG (all Siemens Healthcare Diagnostics GmbH).

Genetic Analyses

A semicustom Axiom myDesign genotyping array (Affymetrix, Santa Clara, CA, USA) was used. Array specifications and quality controls have been described in detail before (9). Principal components were generated using GCTA (v1.24) (14) and genetic outliers were excluded based on inspection of the first two principal components. Genomic inflation was calculated using PLINK (v1.07) (15) to ensure minimization of population stratification, excluding SNPs in the complex major histocompatibility complex (MHC) region (chromosome 6, 29–33 MB). PLINK also was used for association testing using the following exclusion criteria: Hardy-Weinberg P <5E-07, minor allele frequency <0.01, missingness per marker >0.05 and missingness per individual >0.02. SNPs on sex chromosomes were excluded from analysis. Variants in high linkage of genome-wide significant SNPs were identified using SNAP Proxy Search (http://www.broadinstitute.org/mpg/snap/) (16), using the 1000 Genomes Pilot 1 CEU population panel and a r^2 threshold of 0.8. Patients with

confirmed diagnosis of borreliosis (N = 100) recruited in Ulm were genotyped using the KASP genotyping system (LGC Genomics, Berlin, Germany) after DNA isolation from blood using the Jetquick Blood and Cell Culture Kit (Genomed, Loehe, Germany).

Cell Culture, Animals, cDNAs, Site-Directed Mutagenesis and Transfection

Human *ANO10* cDNA (NM_018075.2) was purchased from OriGene (SC113757, Rockville, MD, USA) and cloned in pcDNA3.1 with a C-terminal His-Tag (Life Technologies [Thermo Fisher Scientific Inc., Waltham, MA, USA]). R263H-ANO10, L510R-ANO10, L384fs-ANO10, LRRC8A and AQP1 were mutated and cloned, respectively, using standard polymerase chain reaction (PCR) techniques. All cDNAs were verified by sequencing. Culturing of HEK293 cells, THP-1 cells and lymphocytes and isolation of mouse macrophages has been described earlier (17). Site-directed mutagenesis, transfection methods and other used constructs have been described previously (18).

Fluorescent *Borrelia*

Red fluorescent *B. garinii* PRJS1009-Cherry were used to infect macrophages. In some experiments, cells were exposed to TNFα (100 ng/mL) for 2–6 h. THP-1 monocytes were differentiated into macrophages by incubation with 100 nmol/L phorbol 12-myristate 13-acetate (PMA) (Sigma-Aldrich, Munich, Germany) for 48 h.

Patch Clamping

Cells grown on cover slips were mounted in a perfused bath on the stage of an inverted microscope (IM35, Zeiss, Munich, Germany) and kept at 37°C The bath was perfused continuously with Ringer solution (145 mmol/L NaCl, 0.4 mmol/L KH_2PO_4, 1.6 mmol/L K_2HPO_4, 6 mmol/L D-glucose, 1 mmol/L $MgCl_2$, 1.3 mmol/L Ca-gluconate, pH 7.4) at about 10 ml/min. Cell swelling was induced by removing 100 mmol/L mannitol from an isotonic (300 mosmol/L) modified Ringer solution to achieve a hypotonic bath solution (Hypo, 33%, 200 mosmol/L). Patch-clamp experiments were performed in the fast whole-cell configuration as described previously (17).

Two-Electrode Voltage Clamp

Oocytes were harvested from *Xenopus* laevis according to German regulations governing animal experiments. Oocytes were defolliculated for 1 h at 18°C with 1.5 mg/mL collagenase type V (Sigma-Aldrich, St. Louis, MO, USA). After washing oocytes were injected with cRNA encoding ANO10, R263H-ANO10 and AQP1. Preparation of cRNA and voltage clamping of the oocytes have been described earlier (17).

Measurement of $(Ca^{2+})_i$

The plasma membrane-bound calcium sensor has been modified by the addition of a N-terminal signal peptide (20 aa) from neuromodulin (Pl-G-CaMP2). Addition of this peptide results in posttranslational palmitoylation of the protein, which facilitates anchoring of the protein to the plasma membrane. HEK293 cells were transfected on coated glass cover slips with pcDNA31 Pl-G-CaMP2 and were mounted in a perfusion chamber 48 h after transfection. Cells were perfused with Ringer solution at a rate of 8 mL/min at 37°C. Cell fluorescence measurements were measured continuously with an inverted microscope Axiovert S100 (Zeiss) using a 40× objective (Fluar 40×/1.3 oil, Zeiss) and a high speed polychromator system (VisiChrome, Visitron, Puchheim, Germany). Pl-G-CaMP2 was excited at 485 nm and 405 nm. Emission was recorded between 520 nm and 550 nm using a CCD-camera (CoolSnap HQ, Visitron). Control of experiments, imaging acquisition and data analysis were done with the software package Meta-Fluor (Universal Imaging, New York, USA). Alternatively, cells were loaded with Fura2 and intracellular Ca^{2+} concentrations were determined as described earlier (17).

Flow Cytometry, Single Cell Volume Measurements and Migration

Cells were washed and redissolved in 10 mL isotonic or hypotonic Ringer solution as described for patch clamp experiments. Cells were analyzed at 37°C/pH 7.4 using a CASY flow cytometer (Roche Diagnostics, Mannheim, Germany). Cells were analyzed at a density of 10^6 cells/mL. For single cell volume measurements cells were loaded with 1 μg of calcein-AM (Molecular Probes [Thermo Fisher Scientific]) and 0.01% pluronic in a standard bath solution (Ringer) for 60 min at 20–22°C. Fluorescence intensity was measured at an excitation wavelength of 485 nm and an emission wavelength of 520–550 nm. Cell swelling and RVD were observed for 10 to 15 min after applying hypotonic bath solution. Cell migration was assessed in Boyden chambers as described previously (17).

Measurement of TNFα Release

THP-1 cells were grown in 96-well plates and, when mentioned, treated with PMA (100 nmol/L) for 2 d. Before sample collection, cells were infected with cherry-labeled *B. garinii* (MOI 1:10) for 4 h at 37°C. Following a centrifugation step, the supernatant was collected and immediately stored at –20°C. TNFα was measured using Platinum ELISA kit (eBioscience Affymetrix, Vienna, Austria) according to the manufacturer's instructions.

Phagocytosis Assay

THP-1 cells were treated with PMA (100 nmol/L) for 2 d. Cells were infected with cherry-labeled *B. garinii* (MOI 1:10) at 37°C. After infection, cells were washed with PBS to remove remaining *Borrelia*. Cells were visualized and fluorescence was detected by using an Axiovert 200 microscope and AxioVision software (Zeiss), and mean fluorescence intensity was quantified.

Annexin V Binding Assay

THP-1 cells treated with PMA (100 nmol/L, 48 h) were grown in a 96-

well plate. Cells were washed twice with cold PBS and incubated with annexin V-FITC for 15 min at room temperature (FITC Annexin V Detection Kit, BD Biosciences, Heidelberg, Germany). Fluorescence intensity was detected using a plate reader (Novostar, BMG Labtech, Ortenberg, Germany). Cells were treated with TNFα (10 ng/mL) or with cherry-labeled *B. garinii* (MOI 1:10) for 4 h, followed by washing with PBS and fluorescence detection, considered as time point zero. For other time points, the cells were washed to remove the remaining *Borrelia* and kept with fresh media for days following infection.

Western Blotting, Biotinylation and Immunocytochemistry

Protein was isolated from THP-1 cells grown in the absence or presence of PMA (100 nmol/L) and transfected with siRNA-ANO10 (ID# s30237, s30238, Ambion, Life Technologies [Thermo Fisher Scientific]). Cells were lysed using lysis buffer containing 150 mmol/L NaCl, 50 mmol/L Tris, 1 mmol/L EDTA, 100 mmol/L DTT, 0,5% NP-40 and 1% protease inhibitor cocktail (Roche, Mannheim, Germany). Protein separation, transfer, blotting and detection have been described previously (17). A polyclonal rabbit anti-Ano10 antibody (Aviva Systems Biology, San Diego, CA, USA) was used at a dilution of 1:500. Rabbit anti β-actin antibody (Sigma-Aldrich) was used at a dilution of 1:1000. For biotinylation of plasma membrane proteins EZ-Link Sulfo-NHS-SS-Biotin (#89881, Pierce, Thermo Fisher Scientific) was prepared at a concentration of 1 mg/mL in ice-cold phosphate-buffered saline (PBS). Biotinylated cells were lysed and 100-µL streptavidin beads (Thermo Fisher Scientific) were added to the supernatant after centrifugation. After incubation overnight at 4°C, beads were washed five times with cold lysis buffer and biotinylated proteins were eluted by boiling the sample for 5 min at 95°C in SDS sample buffer. For immunocytochemistry of ANO10, the anti-ANO10 antibody was used at a dilution of 1:500.

Table 1. Cross-sectional prevalence of anti-*Borrelia* antibodies.

Study group	Anti-*Borrelia* AB status, N (%)			*P* (Pearson χ^2)[a]
	Seropositive	Seronegative	Total	
GRAS patients (schizophrenia)	85 (7.9)	991 (92.1)	1,076 (100)	0.05
Affective disorder patients[b]	16 (10.8)	132 (89.2)	148 (100)	0.07
GRAS controls (healthy subjects)	68 (5.4)	1,203 (94.6)	1,271 (100)	
Total	169 (6.8)	2,326 (93.2)	2,495 (100)	

[a]Corrected for age and sex. *P* values represent results of χ^2 tests, comparing the respective patient sample with healthy controls.
[b]Included are patients with monopolar or bipolar depression.

Statistics

Group differences in categorical and continuous variables were assessed using chi-square (χ^2 or Mann-Whitney *U* tests. A generalized linear model was employed upon covariate inclusion. At normal distribution of continuous variables, *t* tests were performed (paired and unpaired tests, respectively, for experiments in oocytes, HEK293 cells, lymphocytes and macrophages). A basic allelic test, implemented in PLINK, was used to test for association between single nucleotide polymorphisms (SNPs) and *Borrelia* serological status. *P* values < 0.05 were considered significant and multiple testing corrected (Bonferroni) where indicated, but are displayed uncorrected. Data in figures are expressed as mean ± SEM, in tables as mean ± SD.

All supplementary materials are available online at www.molmed.org.

RESULTS

Borrelia Seropositivity in Health and Neuropsychiatric Disease

We detected anti-*Borrelia* antibodies (AB) in 169 out of 2,495 individuals in total (6.8%) (Table 1). AB prevalence tended to be higher in schizophrenia patients (7.9%, *P* = 0.05) and affective disorder patients (11.0%, *P* = 0.07), when compared with psychiatrically healthy controls (5.4%). *P* values are corrected for sex and age since male subjects are more likely to be seropositive than females (8.2% versus 4.3%, *P* = 1.96E-04, odds ratio (OR) = 1.98, Supplementary Table S1). Furthermore, groups differ significantly in mean age (Supplementary Table S2), which has to be considered because the likelihood of a past *Borrelia* infection and subsequent antibody formation increase with age (Supplementary Figure S1). We did not find a difference in mean titer levels of seropositive subjects between patient groups and controls (Supplementary Table S3). Overall, seropositive and seronegative schizophrenia patients do not show differences with respect to major disease phenotypes of schizophrenia including neurological signs as determined by the CNI, which should also cover symptoms of borreliosis (Supplementary Table S4). Interestingly, however, AB carriers score significantly worse throughout all scales of the BSI (corrected for age and sex as a proxy for gender) (13), an instrument based on patients' self-evaluation (Supplementary Figure S2).

GWAS on *Borrelia* Antibody Seropositivity

In a principal component analysis, 19 subjects showed non-European ancestry and were consequently excluded from genetic analyses (Supplementary Figure S3). We finally analyzed a total of 2,376 individuals with available complete genotype and serological data, fulfilling all inclusion criteria. Of these, 162 (6.8%) were seropositive and 2,214 (93.2%) seronegative. With the use of an allelic model, 580,108 autosomal SNPs were tested and genomic inflation was low (λ = 1.016, Supplementary Figure S4). Two SNPs (rs17850869, rs41289586) exceeded the threshold for genome-wide significance, when correcting for the number of tested

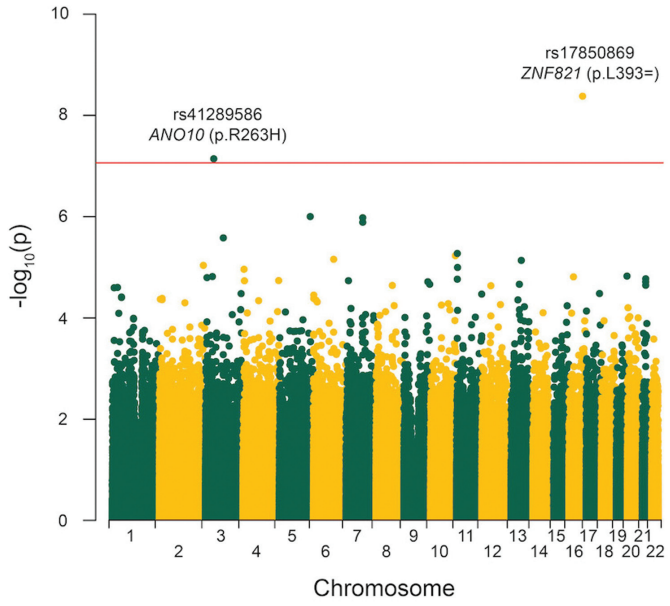

Figure 1. Manhattan plot of genome-wide association analysis. The red horizontal line designates the threshold for genome-wide significance, corrected for number of tested SNPs.

SNPs (P = 8.62E-08, Figure 1). A list of 11 SNPs with P <1.0E-05 is provided as Supplementary Table S5, including minor allele frequencies, association statistics, positions and SNP classifications.

Genome-Wide Significant Hits

Both genome-wide significant SNPs show a low minor allele frequency in seronegative subjects, which is significantly higher in AB carriers (rs17850869: 0.008 versus 0.043; rs41289586: 0.022 versus 0.071, Supplementary Table S5). Genotype distributions are presented in Table 2, where we also display results using additional open-access resources from the 1000 Genomes Project (19) and the Exome Variant Server [NHLBI GO Exome Sequencing Project (ESP); (20)]. Overall, these data are highly similar to the distribution in our seronegative population; hence an underrepresentation of the minor alleles is unlikely to be the source of association. As an exception, the minor allele frequency (MAF) of rs17850869 is higher in the European 1000 Genomes Project study participants (MAF = 0.022). This may, however, be a bias of the small number of individuals included there (Table 2).

One of the two genome-wide significant SNPs, rs17850869, is a synonymous coding variant of zinc finger protein 821, encoded by the *ZNF821* gene on chromosome 16 (NP_001188482.1, p.Leu393) and associated with a P value of 4.17E-09 (OR = 5.36). It is in complete linkage with only one other SNP, rs74944699, an intronic variant in *PMFBP3*. Of note, the gene upstream of *ZNF821* is *ATXN1L* (ataxin 1-like), a paralog of *ATXN1* (ataxin 1), which is associated with spinocerebellar ataxia type 1 (SCA1) (21).

The other SNP, rs41289586 (P = 7.18E-08, OR = 3.38), is a missense variant of anoctamin 10, encoded by the gene *ANO10* (NP_060545.3, p.R263H) on chromosome 3. It shows linkage (r^2 > 0.8) with two intronic SNPs, rs62250916 in *ANO10* and rs11926254 in *SNRK*. With the use of software tools for a prediction of the effect of amino acid substitutions on protein function, the ANO10-R263H variant was predicted to be "probably damaging" (score 1.000) by PolyPhen-2 (http://genetics.bwh.harvard.edu/pph2/) (22), "deleterious" (score –4.66) by PROVEAN and "damaging" (score 0.000) by SIFT (both http://provean.jcvi.org/) (23,24). Notably, also mutations in *ANO10* were reported to be causative for spinocerebellar ataxia (25,26).

Table 2. Genotypes and MAFs of GWAS hits.[a]

Subjects or populations according to reference SNP ID	Genotypes			MAF	P[b] (allelic test) (OR, (95% CI))
	CC	CT	TT		
rs17850869					
Seropositive	148	14	0	0.043	
Seronegative	2,177	37	0	0.008	4.17E–09 (5.36, (2.87–10.02))
1000g (CEU)	80	5	0	0.029	0.449 (1.49, (0.53–4.21))
1000g (EUR)	362	17	0	0.022	0.061 (1.97, (0.96–4.04))
EVS (EA)	4,148	50	2	0.006	1.50E–13 (6.98, (3.84–12.70))
rs41289586					
Seropositive	140	21	1	0.071	
Seronegative	2,118	96	1	0.022	7.18E–08 (3.38, (2.11–5.39))
1000g (CEU)	80	5	0	0.029	0.058 (2.52, (0.94–6.76))
1000g (EUR)	362	17	0	0.022	1.1E–04 (3.33, (1.75–6.32))
EVS (EA)	4,074	222	4	0.027	2.47E–06 (2.78, (1.78–4.33))

CI, confidence interval; 1000g, 1000 Genomes Project; CEU, Utah Residents (CEPH) with Northern and Western European ancestry panel; EUR, European superpopulation panel; EVS (EA), Exome variant server European American population panel.

[a]Genotype distribution of GWAS hits in seropositive versus seronegative subjects, as well as in additional control populations.

[b]P values represent results of allelic tests, comparing the respective control sample with the seropositive subjects.

We investigated, but did not find, an association of either SNP with antibodies against several other bacterial infections (*Helicobacter pylori*, *Mycoplasma pneumoniae*, *Chlamydia pneumoniae*, *Chlamydia trachomatis*). They also were not associated with a sum score including all five serological tests against bacterial infections in a linear regression model (Supplementary Table S6). Neither SNPs is found on commonly used genotyping arrays and were thus not included previously in GWAS investigating other phenotypes. In our study cohort, they were not associated with the diagnosis of schizophrenia (rs41289586: $P_{allelic} = 0.11$, rs17850869: $P_{allelic} = 0.28$).

Compromised Cellular Volume Regulation by ANO10-R263H

ANO10 belongs to a family of 10 proteins which operate as Cl^- channels and phospholipid scramblases (27–31). Structural insights into TMEM16/anoctamin proteins were provided recently (32). R263 is located close to the dimer interface and is well conserved within the anoctamin family and between species (Supplementary Figures S8B, C). Anoctamins have been reported earlier to be relevant for cellular volume regulation (18,33,34), which is essential for cell migration and immune defense (35). Anoctamins may be part of a channel or regulatory complex that produces volume-regulated anion currents (I_{Hypo}) activated by hypotonic bath solution (Hypo). An essential component of such a complex has been identified as LRRC8 (36,37). We examined the role of ANO10 for volume regulation by coexpression with aquaporin 1 in *Xenopus* oocytes, which swell and eventually burst when exposed to Hypo (38). Expression of ANO10, but not R263H-ANO10, produced large outwardly rectifying whole cell currents (I_{Hypo}) when oocytes were exposed to Hypo (Figures 2A, B). Coexpression of R263H-ANO10 together with ANO10 suppressed activation of I_{Hypo} (Figure 2C). Moreover, bursting of oocytes due to Hypo-induced swelling was reduced by ANO10 but not by R263H-ANO10 (Figure 2D). It is worth noting that activation of phospholipase A2 by melittin, a known activator of I_{Hypo}, also activated ANO10. Moreover, coexpression of LRRC8A, which itself induced I_{Hypo}, did not further augment I_{Hypo} produced by ANO10 (Figures 2E, F). Taken together, ANO10 but not R263H-ANO10 generates swelling-activated whole cell currents in oocytes.

We also expressed ANO10 in HEK293 cells and found enhanced whole cell currents activated by Hypo, which were inhibited by typical anoctamin blockers such as NPPB, NS3728 and $T_{inh}A01$ (Figures 3A, B). Currents could not be activated in the complete absence of Ca^{2+}, but were augmented, along with an increase in volume regulation (regulatory volume decrease, RVD), when only extracellular Ca^{2+} was reduced to 0.1 μmol/L (Figure 3C, Supplementary Figures S5A, B). I_{Hypo} was inhibited by arachidonic acid, confirming earlier reports (39) and was controlled by phospholipase A2 (Supplementary Figures S5C–F). Notably, I_{Hypo} was significantly reduced by the expression of two ANO10-mutants that have been reported to cause cerebellar ataxia (25,26) (Supplementary Figures S5G, H). Expression of ANO10 augmented RVD during exposure to Hypo when measured by flow cytometry or single cell imaging of calcein-loaded cells (Figures 3D–G). These data establish a role of ANO10 for volume regulation in mammalian cells.

In contrast to (wild-type) wt ANO10, R263H-ANO10 failed to produce large I_{Hypo} and compromised RVD in HEK293 cells (Figures 4A–C). Virtually identical results were obtained when ANO10 and R263H-ANO10 were expressed in lymphocytes (Supplementary Figure S6). Immunocytochemistry and membrane biotinylation showed weak membrane expression of ANO10 and R263H-ANO10 and suggested primarily a location of ANO10 in the endoplasmic reticulum (ER) (Figures 4H–J). Using the plasma membrane-targeted Ca^{2+}-sensitive protein GCAMP2 (Figures 4D, E), or conventional Fura2 imaging (Figure 4F), we found that Hypo induced a delayed transient rise in intracellular Ca^{2+}, which was augmented by ANO10 but reduced by R263H-ANO10. However, ANO10 does not seem to affect the filling of the ER Ca^{2+} store, since the SERCA pump inhibitor cyclopiazonic acid (CPA) induced a similar Ca^{2+} increase in the absence or presence of ANO10 (Figure 4G). Hypo-induced store release occurred through dantrolene-sensitive ryanodine receptors (40). In the presence of dantrolene, I_{Hypo} was not augmented by ANO10 (Supplementary Figure S5I, J). Taken together, R263H-ANO10 may compromise volume regulation by participating in an ion channel complex or by controlling intracellular Ca^{2+} signaling (Supplementary Figure S8A).

Compromised Macrophage Function in the Absence of ANO10

Macrophages are within the first line of defense during infection with *Borrelia* (41). We found that ANO10 is expressed along with ANO6 in human THP-1 macrophages as well as in freshly isolated mouse peritoneal macrophages (Figures 5A, B; Supplementary Figures S7A, B). In THP-1 macrophages, ANO10 was located mostly intracellularly (Figure 5C). RVD was examined in single cells by loading macrophages with calcein. Recovery from Hypo-induced cell swelling (RVD) was reduced after siRNA-knockdown of ANO10 (Figures 5D, E). Similar results were obtained in mouse macrophages in which Ano10 expression was inhibited by siRNA or was knocked down in $Ano10^{lox/lox}$/E2A-cre mice (Supplementary Figures S7C–E). The results indicate that ANO10 is important for volume regulation also in human and mouse macrophages.

Similar to the experiments in oocytes, in macrophages, expression of ANO10-R263H inhibited I_{Hypo} (Figure 5F). I_{Hypo} and volume regulation is a prerequisite for cell migration and thus crucial for eradication of spirochetes (35,42). We therefore examined migration of macrophages, which was induced by monocyte chemoattractant protein 1

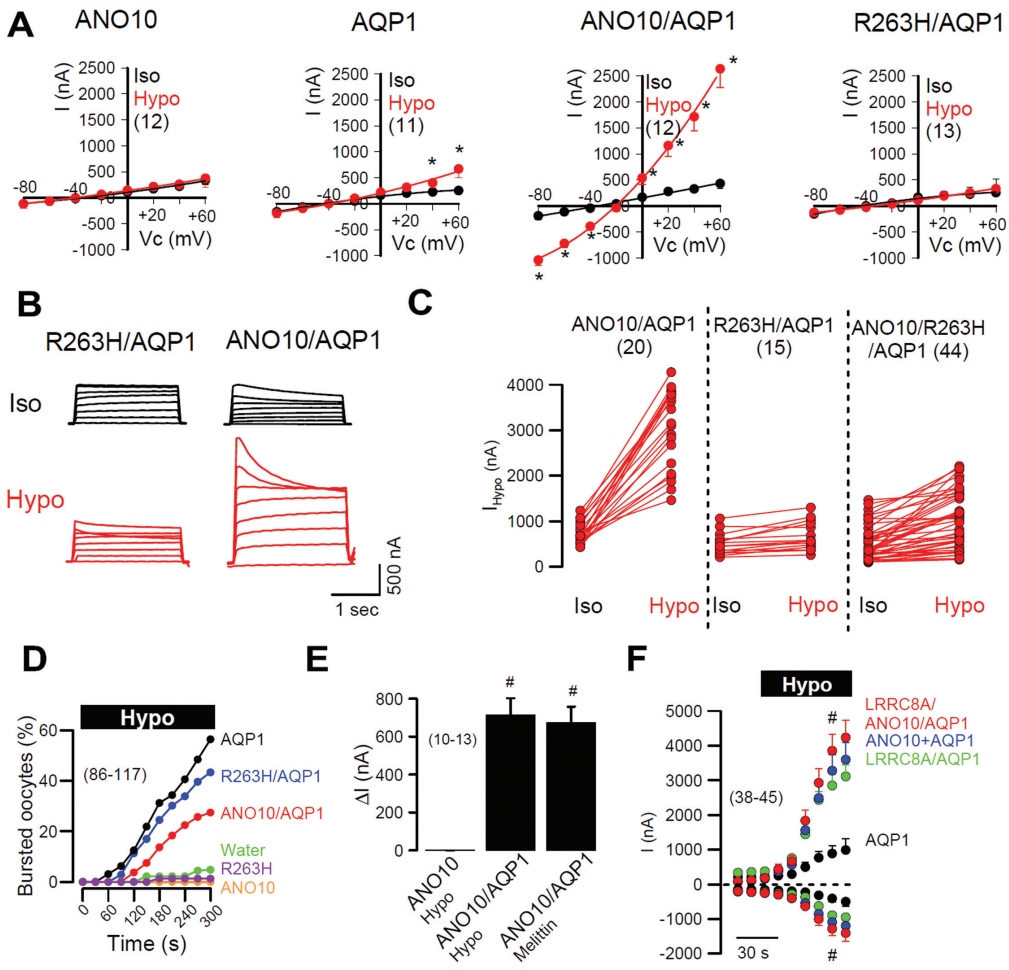

Figure 2. ANO10 but not R263H-ANO10 generates volume-activated whole cell currents in *Xenopus* oocytes. (A) Current–voltage relationships of whole cell currents activated by cell swelling (I_{Hypo}, 50 % reduced extracellular osmolarity) in *Xenopus* oocytes. R263H-ANO10 does not produce I_{Hypo}. (B) Current overlay (voltage clamp (Vc) = ±100 mV) demonstrates typical time dependent inactivation of I_{Hypo}. (C) I_{Hypo} in oocytes expressing (left to right, respectively): AQP1 and ANO10; AQP1 and ANO10-R263H; or AQP1, ANO10, and ANO10-R263H. Coexpression of ANO10-R263H suppressed currents produced by wt ANO10. (D) Oocyte bursting after exposure to hypotonic bath solution. Fraction of burst oocytes was reduced by expression of ANO10. Oocytes survived in the absence of AQP1. (E) Summary of whole cell currents activated by Hypo and the PLA_2-activator melittin (100 nmol/L). (F) Summary of time-dependent activation of whole cell currents in cells expressing ANO10, LRRC8A or coexpressing both. All oocytes expressed AQP1. Mean ± SEM (number of oocytes); *significant activation by Hypo (paired *t* test); #significant difference (by unpaired *t* test) when compared with ANO10 alone (E) or with ANO10 plus AQP1 (ANO10+AQP1) (F).

(MCP-1). Migration was largely reduced by siRNA-knockdown of ANO10 and was inhibited by typical anoctamin blockers (Figure 5G). Cell viability was not affected by these procedures (data not shown). Because cell migration and phagocytic activity of macrophages will determine the efficacy of spirochete eradication (35,42), we examined phagocytosis of red-fluorescent cherry-labeled *B. garinii* by THP-1 macrophages. Phagocytosis of *B. garinii* was reduced significantly after siRNA-knockdown of ANO10 (Figures 5H, I). Exposure to *B. garinii* induced a strong release of the major cytokine TNFα by THP-1 cells, which was not affected by knockdown of ANO10 (Figures 5J, K). No immediate cell death was observed upon exposure and phagocytosis of *B. garinii*, but apoptosis of THP-1 macrophages was reduced 6 d after exposure to *B. garinii*, which may allow *B. garinii* to circumvent innate defense (data not shown). Taken together, the present results suggest that ANO10 is important for volume regulation of macrophages and for their role in innate immunity. Eradication of spirochetes may be compromised in carriers of the ANO10 variant R263H.

Phenotypes in Borreliosis Patients

In a subsequent exploratory human study, we wondered whether patients with laboratory-confirmed borreliosis, carrying the ANO10-R263H variant

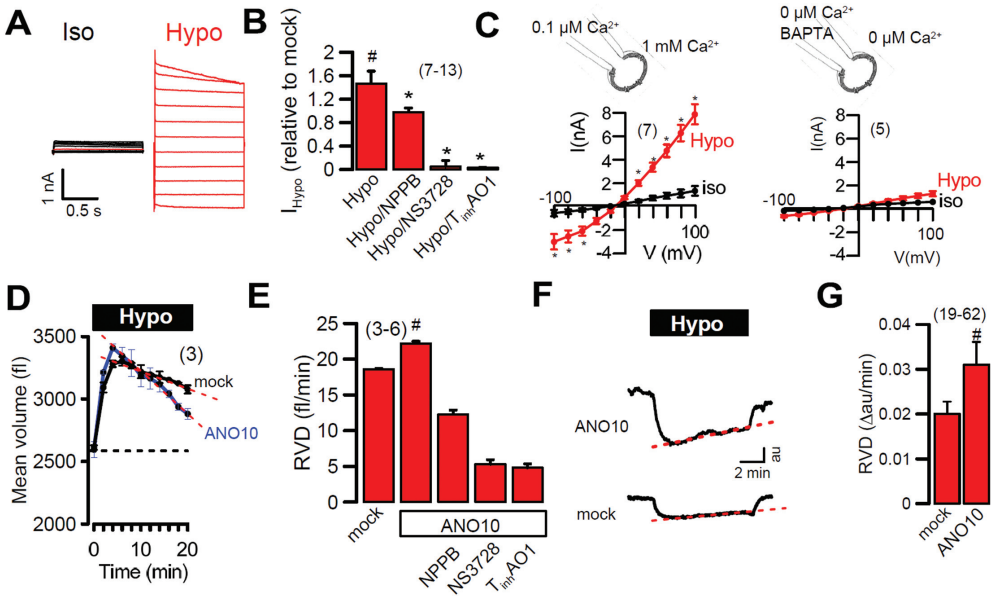

Figure 3. ANO10 affects volume-activated whole cell currents in HEK293 cells. (A) Whole cell currents (voltage clamp (Vc) = ± 100 mV) activated by cell swelling (I_{Hypo}, 33% reduced extracellular osmolarity) in ANO10-expressing cells. (B) Swelling induced currents (I_{Hypo}) in ANO10-expressing cells relative to mock transfected cells and inhibition by NPPB (50 µmol/L), NS3728 (5 µmol/L) and T_{inh}AO1 (20 µmol/L). (C) Current–voltage (I–V) curves indicating loss of I_{Hypo} with complete elimination of Ca^{2+} and preincubation with BAPTA (1,2-bis(o-aminophenoxy)ethane-*N,N,N′,N′*-tetraacetic acid; 50 µmol/L, 30 min). (D) Regulation of cell volume in the presence of Hypo (regulatory volume decrease, RVD) in mock-transfected cells or cells overexpressing ANO10 (flow cytometry). (E) RVD in mock-transfected cells or cells overexpressing ANO10 and inhibition by NPPB, NS3728 and T_{inh}AO1. (F) Reshrinkage of cells exposed to hypotonic bath solution (RVD), measured in single cells loaded with calcein. (G) Comparison of RVD (measured by calcein fluorescence) obtained in mock-transfected and ANO10-overexpressing cells. Mean ± SEM (number of cells); *significant inhibition (paired *t* test); #significant difference to mock (unpaired *t* test).

would differ in any respect from noncarriers. Specifically, due to the potential association of both identified SNPs with cerebellar ataxia, we searched for a potential overrepresentation of cerebellar ataxia-like symptoms that also have been reported previously in cases of neuroborreliosis (43). To address this question, we recruited prospectively 100 patients with laboratory-confirmed diagnosis of borreliosis. Patients had a mean age of 56.3 years (standard deviation: 16.0 years, range: 15 to 86 years), 58% were male. Classical clinical correlates of neuroborreliosis (including meningitis, radiculitis, cranial nerve palsy, ataxia, dizziness, encephalitis) were present in 30 patients and those of systemic Lyme borreliosis (including erythema migrans, arthralgia, myalgia, headache, malaise, nausea, dizziness) were present in 20 patients. A total of 50 patients had just a laboratory-based diagnosis without typical clinical signs and symptoms; 4 out of this total of 100 individuals carried the rs41289586 risk allele (T, ANO10-R263H variant) and 2 of 100 had the rs17850869 risk allele (T); all were heterozygous (CT) for these risk SNPs. Of the 6 (4 + 2) risk allele carriers, 5 had the diagnosis borreliosis without typical clinical symptoms (only laboratory signs of infection) in contrast to 45 of 94 noncarriers (5 of 6 versus 45 of 94: Fisher exact $P = 0.20$). Moreover, 3 of 6 had cerebellar symptoms in contrast to 28 of 94 (3 of 6 versus 28 of 94: Fisher exact $P = 0.37$). Apart from these potentially interesting hints that would need to be consolidated in larger followup studies, no prominent clinical differences were detected.

DISCUSSION

In the first GWAS on *Borrelia* antibody serostatus, we identified two host genomic variants mediating differential susceptibility to *Borrelia* seropositivity. Interestingly, both variants, located on chromosomes 3 and 16, happen to be in some context with spinocerebellar ataxia (25,26). The SNP on chromosome 3, rs41289586, represents the missense variant ANO10-R263H, encoded by the gene *ANO10*. We provide here first evidence of this variant modifying normal host defense. The role of the variant on chromosome 16, rs17850869, a synonymous SNP in *ZNF821* is presently less clear. Addressing the second objective of the present study, that is, to potentially relate *Borrelia* seropositivity to core phenotypes of neuropsychiatric disorders, we obtained a significantly higher symptom load of seropositive versus seronegative individuals in essentially all items of the BSI (13) self-rating scale.

Macrophage function is essential for eradication of *Borrelia* (41). We recently found a role of anoctamin 6 (ANO6) for

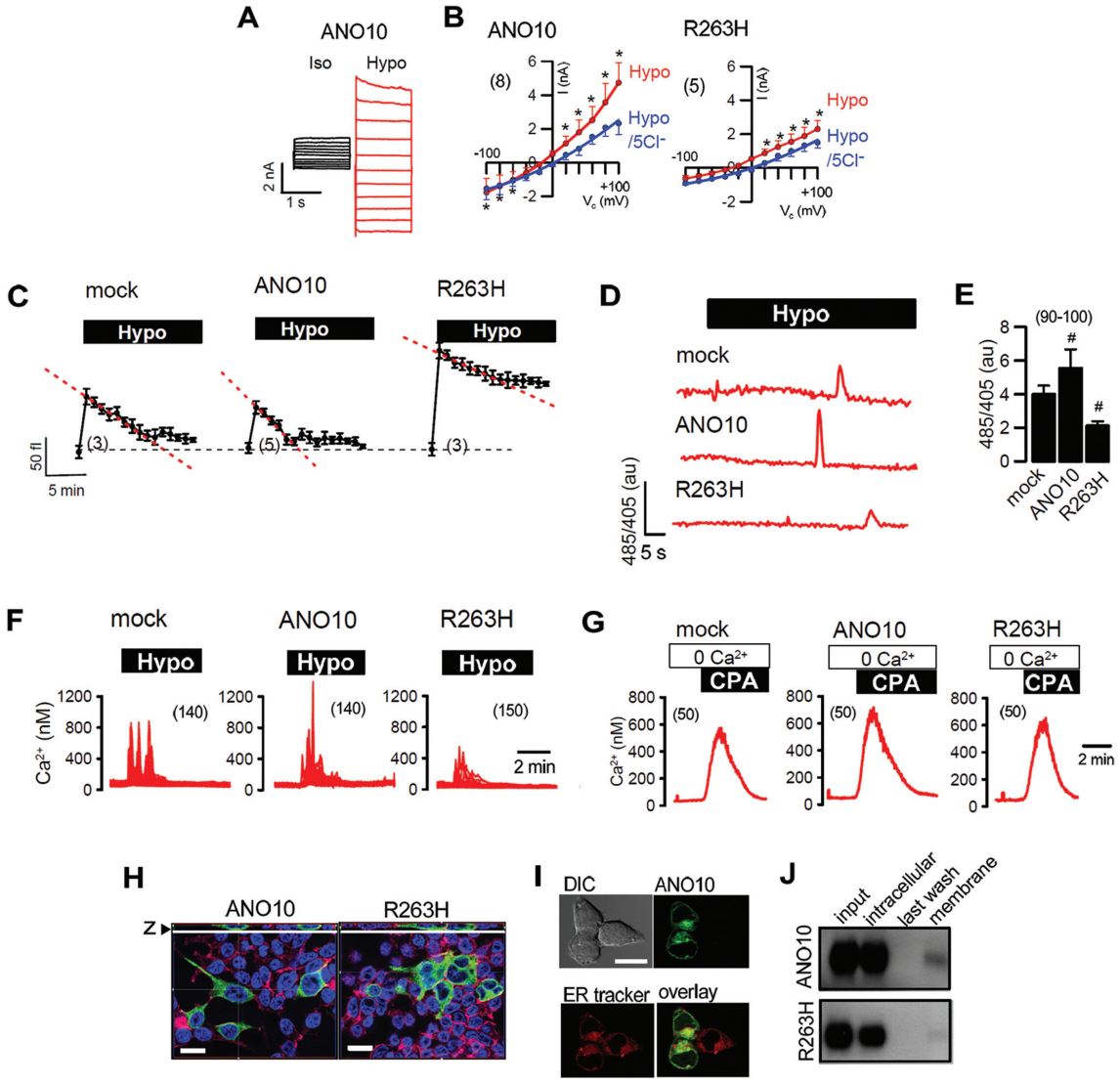

Figure 4. R263H inhibits volume regulation, I_{Hypo} and intracellular Ca^{2+} signaling in HEK293 cells. (A) Whole cell currents (voltage clamp (Vc) = ± 100 mV) activated by cell swelling (I_{Hypo}, 33 % reduced extracellular osmolarity) in cells expressing ANO10 and R263H-ANO10 (R263H). (B) Current–voltage relationships for I_{Hypo} and inhibition of I_{Hypo} by removal of Cl^- from the extracellular bath solution ($5Cl^-$). (C) Regulation of cell volume in the presence of Hypo (regulatory volume decrease, RVD) in cells expressing ANO10 or R263H (flow cytometry). (D) Effect of cell swelling on intracellular (Ca^{2+}) in cells expressing ANO10 or R263H or mock transfected cells, as measured by the Ca^{2+} sensor GCAMP2. (E) Summary of the effects of cell swelling on $(Ca^{2+})_i$ (485/405 fluorescence emission ratio) in ANO10 and R263H expressing cells. (F) Collected recordings of the effects of cell swelling on $(Ca^{2+})_i$, measured by Fura2. (G) Collected recordings of the effects of ER-store emptying by cyclopiazonic acid (CPA; 10 μmol/L) on $(Ca^{2+})_i$, measured by Fura2. (H) Confocal images of cells expressing ANO10 or R263H suggesting weak membrane expression. (I) Live staining of ANO10-GFP (green) and ER (ER-tracker; red) suggesting ER localization of ANO10. (J) Membrane biotinylation of cells expressing ANO10 or R263H, suggesting low membrane expression of ANO10, which is even reduced for R263H. Mean ± SEM (number of experiments); #significant difference when compared with mock (analysis of variance (ANOVA)); §significant difference when compared with ANO10 (ANOVA). Bar = 20 μm. Numbers are given in the graph in parenthesis. z, z-scan, side view; DIC, differential interference contrast.

immune functions of macrophages (17), while volume regulation by anoctamins has been reported earlier (18,33,34). We therefore analyzed the role of ANO10 for volume regulation and found that I_{Hypo} and RVD are depending on ANO10 in oocytes, HEK293 cells, lymphocytes and macrophages. The properties of ANO10-induced I_{Hypo} correspond well to those described for VRAC (reviewed in [44–46]). How does ANO10 control I_{Hypo} and thereby affect RVD? It could be a

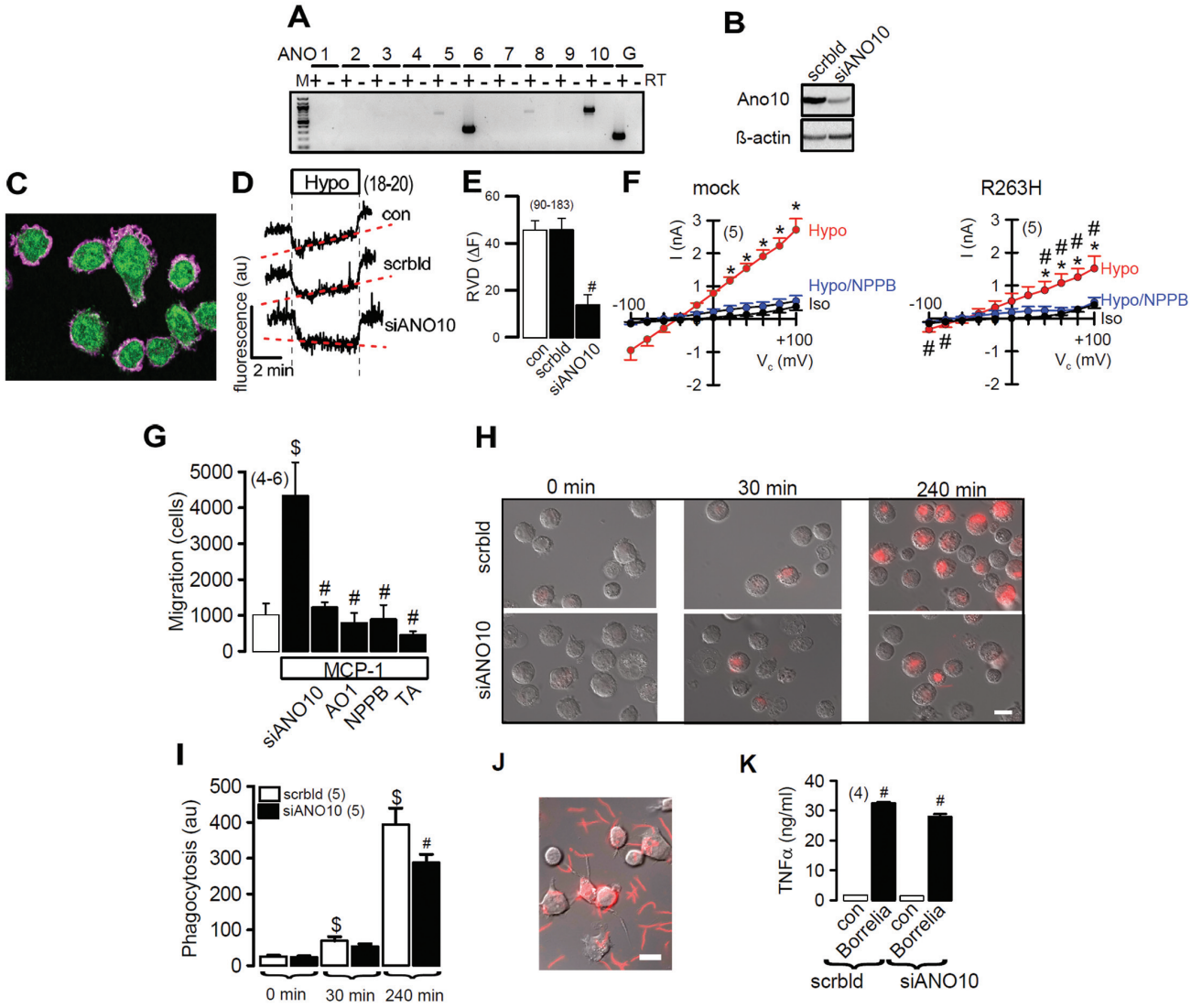

Figure 5. Role of ANO10 for volume regulation in macrophages. (A) RT-PCR analysis of anoctamin expression in THP-1 macrophages. (B) Western blot indicating knockdown of ANO10-expression by siRNA. (C) ANO10 (green) and peripheral actin (rhodamin-phalloidin) of THP-1 cells suggesting dominant intracellular location of ANO10. (D) Summary trace for reshrinkage of cells exposed to hypotonic bath solution (RVD), measured in single cells loaded with calcein. RVD was abolished after siRNA-knockdown of ANO10. (E) Summary of RVD measured by absolute fluorescence change. (F) I/V curves indicating reduced I_{Hypo} in R263H-expressing cells. (G) Migration assay in Boyden chambers. MCP-1 induced migration was inhibited by siRNA knockdown of ANO10 and anoctamin inhibitors T_{inh}AO1 (20 μmol/L), NPPB (50 μmol/L) or tannic acid (TA, 10 μmol/L). (H) THP-1 cells exposed to red-fluorescent cherry-labeled *B. garinii*. Accumulation of cytosolic fluorescence, indicating progressing phagocytosis of *Borrelia* by THP-1 cells. (I) Increase in fluorescence intensity as a measure of phagocytic activity. (J) Exposure of THP-1 cells to cherry-labeled *B. garinii*. (K) Release of TNFα upon exposure to *B. garinii* was not affected by siRNA-knockdown of ANO10. Mean ± SEM (number of cells or assays). #Significant difference when compared with scrambled, MCP-1 alone, mock or con (ANOVA); §significant increase in migration and phagocytosis, respectively (unpaired *t* test). M, marker; RT, reverse transcriptase; con, control; crbld: scrambled control RNA; siANO10: siRNA against ANO10. Bar = 20 μm.

binding partner of the essential VRAC component LRRC8A (36,37), although we did not find a potentiation of I_{Hypo} by co-expression of ANO10 and LRRC8A in oocytes and in HEK293 cells exogenous LRRC8A was even inhibitory on I_{Hypo}. Interestingly, no I_{Hypo} was found when we expressed a LRRC8A mutant lacking the leucine-rich repeat (LRCC8A-D367stop; data not shown), suggesting a role of the LRR-motif for I_{Hypo}. Moreover, LRCC8A-D367stop inhibited ionomycin-activation (1 μmol/L) of endogenous xANO1 currents by 43% ± 5.8% (n = 27) and abolished I_{Hypo} in ANO10 expressing oocytes.

This suggests a functional relationship between LRRC8A and anoctamins. ANO10 also may control compartmentalized Ca^{2+} signals that have been shown to be important for activation of I_{Hypo} (40,47).

R263H-ANO10 had a dominant negative effect on this ANO10 function. Due to the location of R263 close to the dimer interface, the mutation could interfere with dimerization of ANO10, thereby affecting biosynthesis and/or protein function (32) (Supplementary Figures S8B, C). R263H compromised volume regulation, migration and phagocytosis, thereby reducing spirochete clearance. Interestingly another member of the anoctamin family, ANO9 (*TMEM16J*), is of potential relevance for the defense against Mycobacteriae, because polymorphisms in the *PKP3-SIGIRR-TMEM16J* gene region were found to be associated with higher susceptibility to tuberculosis (48).

Notably, mutations in ANO10 were found to cause spinocerebellar ataxia (25,26), which is also a reported phenotype of neuroborreliosis (43). Similar to R263H, these mutations also inhibited I_{Hypo} in our present report. We may speculate that ANO10-R263H and putative further variants convey a genetic predisposition to cerebellar ataxia, possibly requiring an additional hit in the form of an infection to trigger symptoms. The second associated SNP, rs17850869, is a synonymous variant in *ZNF821*. As mentioned earlier, the gene upstream of *ZNF821* is *ATXN1L* (ataxin 1-like), a paralog of *ATXN1* (ataxin 1), which is associated with spinocerebellar ataxia type 1 (SCA1) (21). In mice, a role of *Atxn1l* in SCA1 pathology was recently demonstrated (49).

Although half of our study participants carry a neuropsychiatric diagnosis, our study design did not allow us to investigate whether *Borrelia* can be (co)causative of these diseases. Serotyping was performed after neuropsychiatric diagnosis and inclusion of the patients in the GRAS cohort. Thus, the increased seroprevalence in neuropsychiatric patients cannot be interpreted as a direct contribution to disease etiology, but rather as disease-related deficits in personal hygiene or increased risk-taking behavior. Furthermore, considering the endemic pattern of *Borrelia* infections (50), the distribution of patient recruitment centers across Germany must also be taken into consideration (8). In contrast to patients, healthy volunteers were mainly from Lower Saxony with a relatively low incidence of borreliosis.

We did not find any evidence for a worse clinical outcome of schizophrenic antibody carriers (independent of genotypes) when compared with seronegative schizophrenia patients with respect to core symptoms of schizophrenia or to neurological deficits, as assessed by trained investigators. However, it is important to remember that antibody seropositivity cannot simply be equated with Lyme disease or neuroborreliosis. Nevertheless, when asked for self-assessment of their overall condition employing the BSI (13) seropositive schizophrenia patients rated more severe symptoms throughout all inventory items including the Global Severity Index (GSI). At this time, we cannot provide a reliable interpretation of this data, but their nonspecific nature may reflect the reputation of *Borrelia* as the "great imitator" (51) and it is well known that subjective symptoms can persist after disappearance of objective criteria (1).

CONCLUSION

Our study identified a novel player in innate immune defense, anoctamin 10, which controls cellular volume and macrophage function. We also show that immune response in humans against *Borrelia* varies according to specific genotypes. In the context of further studies, this might help design personalized therapeutic approaches. It is more and more evident that the identification of both virulence factors of the pathogen and susceptibility variants of the host is critical for our understanding of host–pathogen interaction. Joint association analyses of both genomes hold great potential to uncover footprints of natural selection, as shown recently for HIV (52) Progress in the isolation and culture of *Borrelia* from human serum might soon bring similar approaches within achievable range (53).

ACKNOWLEDGMENTS

This work was supported by the Max Planck Society and the Max Planck Förderstiftung, as well as by the DFGSFB699A12, DFG KU756/12-1, Volkswagenstiftung AZ 87499 and the Niedersachsen-Research Network on Neuroinfectiology (N-RENNT) of the Ministry of Science and Culture of Lower Saxony. This work was also supported by a Young Investigator Grant from the Brain & Behavior Research Foundation, as well as a postdoctoral scholarship from the Daimler and Benz Foundation, both awarded to C Hammer.

DISCLOSURE

The authors declare that they have no competing interests as defined by *Molecular Medicine*, or other interests that might be perceived to influence the results and discussion reported in this paper.

REFERENCES

1. Shapiro ED. (2014) Clinical practice. Lyme disease. *N. Engl. J. Med*. 370:1724–31.
2. Stanek G, Wormser GP, Gray J, Strle F. (2012) Lyme borreliosis. *Lancet*. 379:461–73.
3. Fallon BA, Nields JA. (1994) Lyme disease: a neuropsychiatric illness. *Am. J. Psychiatry*. 151:1571–83.
4. Hess A.*et al*. (1999) Borrelia burgdorferi central nervous system infection presenting as an organic schizophrenialike disorder. *Biol. Psychiatry*. 45:795.
5. Hanincova K, *et al*. (2013) Multilocus sequence typing of Borrelia burgdorferi suggests existence of lineages with differential pathogenic properties in humans. *PLoS ONE*. 8:e73066.
6. Casjens SR, *et al*. (2012) Genome stability of Lyme disease spirochetes: comparative genomics of Borrelia burgdorferi plasmids. *PLoS ONE*. 7:e33280.
7. Chapman SJ, Hill AV. (2012) Human genetic susceptibility to infectious disease. *Nat. Rev. Genet*. 13:175–88.
8. Ribbe K, *et al*. (2010) The cross-sectional GRAS sample: a comprehensive phenotypical data collection of schizophrenic patients. *BMC Psychiatry*. 10:91.
9. Hammer C, *et al*. (2014) Neuropsychiatric disease relevance of circulating anti-NMDA receptor autoantibodies depends on blood-brain barrier integrity. *Mol. Psychiatry*. 19:1143–9.

10. World Medical Association. (2013) World Medical Association Declaration of Helsinki: ethical principles for medical research involving human subjects. *JAMA*. 310: 2191–4.
11. (2000) *Diagnostic and Statistical Manual of Mental Disorders: DSM-IV-TR*. 4th edition, text revision. Washington, DC: American Psychiatric Association. 943 pp.
12. Begemann M.*et al*. (2010) Modification of cognitive performance in schizophrenia by complexin 2 gene polymorphisms. *Arch. Gen. Psychiatry*. 67:879–88.
13. Franke GH. (2000) *BSI: Brief Symptom Inventory von L. R. Derogatis*. Göttingen: Beltz.
14. Yang J, Lee SH, Goddard ME, Visscher PM. (2011) GCTA: a tool for genome-wide complex trait analysis. *Am. J. Hum. Genet*. 88:76–82.
15. Purcell S, *et al*. (2007) PLINK: a tool set for whole-genome association and population-based linkage analyses. *Am. J. Hum. Genet*. 81:559–75.
16. Johnson AD, *et al*. (2008) SNAP: a web-based tool for identification and annotation of proxy SNPs using HapMap. *Bioinformatics*. 24:2938–9.
17. Ousingsawat J, *et al*. (2015) Anoctamin 6 mediates effects essential for innate immunity downstream of P2X7-receptors in macrophages. *Nat. Commun*. 6:6245.
18. Almaca J, *et al*. (2009) TMEM16 proteins produce volume-regulated chloride currents that are reduced in mice lacking TMEM16A. *J. Biol. Chem*. 284:28571–8.
19. Abecasis GR, *et al*. (2012) An integrated map of genetic variation from 1,092 human genomes. *Nature*. 491:56–65.
20. Exome Variant Server, NHLBI GO Exome Sequencing Project (ESP) [Internet]. Seattle, WA; [cited 2014 Jul 17]. Available from: http://evs.gs.washington.edu/EVS/
21. Zoghbi HY, Orr HT. (2009) Pathogenic mechanisms of a polyglutamine-mediated neurodegenerative disease, spinocerebellar ataxia type 1. *J. Biol. Chem*. 284:7425–9.
22. Adzhubei IA, *et al*. (2010) A method and server for predicting damaging missense mutations. *Nat. Methods*. 7:248–9.
23. Choi Y, Chan AP. (2015) PROVEAN web server: a tool to predict the functional effect of amino acid substitutions and indels. *Bioinformatics*. 2015, Apr 6 [Epub ahead of print].
24. Kumar P, Henikoff S, Ng PC. (2009) Predicting the effects of coding non-synonymous variants on protein function using the SIFT algorithm. *Nat. Protoc*. 4: 1073–81.
25. Chamova T, *et al*. (2012) ANO10 c.1150_1151del is a founder mutation causing autosomal recessive cerebellar ataxia in Roma/Gypsies. *J. Neurol*. 259:906–11.
26. Vermeer S, *et al*. (2010) Targeted next-generation sequencing of a 12.5 Mb homozygous region reveals ANO10 mutations in patients with autosomal-recessive cerebellar ataxia. *Am. J. Hum. Genet*. 87:813–9.
27. Yang YD, *et al*. (2008) TMEM16A confers receptor-activated calcium-dependent chloride conductance. *Nature*. 455:1210–5.
28. Schroeder BC, Cheng T, Jan YN, Jan LY. (2008) Expression cloning of TMEM16A as a calcium-activated chloride channel subunit. *Cell*. 134:1019–29.
29. Caputo A, *et al*. (2008) TMEM16A, A Membrane Protein Associated With Calcium-Dependent Chloride Channel Activity. *Science*. 322:590–4.
30. Suzuki J, Umeda M, Sims PJ, Nagata S. (2010) Calcium-dependent phospholipid scrambling by TMEM16F. *Nature*. 468:834–8.
31. Malvezzi M, *et al*. (2013) Ca(2+)-dependent phospholipid scrambling by a reconstituted TMEM16 ion channel. *Nat. Commun*. 4:2367.
32. Brunner JD, *et al*. (2014) X-ray structure of a calcium-activated TMEM16 lipid scramblase. *Nature*. 516:207–12.
33. Martins JR, *et al*. (2011) Anoctamin 6 is an essential component of the outwardly rectifying chloride channel. *Proc. Natl. Acad. Sci. U. S. A*. 108:18168–72.
34. Juul CA, *et al*. (2014) Anoctamin 6 differs from VRAC and VSOAC but is involved in apoptosis and supports volume regulation in the presence of Ca. *Pflugers Arch*. 466:1899–910.
35. Schwab A, Fabian A, Hanley PJ, Stock C. (2012) Role of ion channels and transporters in cell migration. *Physiol. Rev*. 92:1865–913.
36. Voss FK, *et al*. (2014) Identification of LRRC8 heteromers as an essential component of the volume-regulated anion channel VRAC. *Science*. 344:634–8.
37. Qiu Z, *et al*. (2014) SWELL1, a Plasma Membrane Protein, Is an Essential Component of Volume-Regulated Anion Channel. *Cell*. 157:447–58.
38. Preston GM, Carroll TP, Guggino WB, Agre P. (1992) Appearance of water channels in Xenopus oocytes expressing red cell CHIP28 protein. *Science*. 256:385–7.
39. Gosling M, Poyner DR, Smith JW. (1996) Effects of arachidonic acid upon the volume-sensitive chloride current in rat osteoblast-like (ROS 17/2.8) cells. *J. Physiol*. 493:613–23.
40. Wu X, *et al*. (1997) Regulatory volume decrease by SV40-transformed rabbit corneal epithelial cells requires ryanodine-sensitive Ca2+-induced Ca2+ release. *J. Membr. Biol*. 158:127–36.
41. Berende A, *et al*. (2010) Activation of innate host defense mechanisms by Borrelia. *Eur. Cytokine Netw*. 21:7–18.
42. Steere AC, Coburn J, Glickstein L. (2004) The emergence of Lyme disease. *J. Clin. Invest*. 113:1093–101.
43. Arav-Boger R, Crawford T, Steere AC, Halsey NA. (2002) Cerebellar ataxia as the presenting manifestation of Lyme disease. *Pediatr. Infect. Dis. J*. 21:353–6.
44. Hoffmann EK, Lambert IH, Pedersen SF. (2009) Physiology of cell volume regulation in vertebrates. *Physiol. Rev*. 89:193–277.
45. Nilius B, *et al*. (1997) Properties of volume-regulated anion channels in mammalian cells. *Prog. Biophys, Mol. Biol*. 68:69–119.
46. Strange K, Emma F, Jackson PS. (1996) *Cell*ular and molecular physiology of volume-sensitive anion channels. *Am. J. Physiol*. 270:C711–30.
47. Lemonnier L.*et al*. (2002) Ca2+ modulation of volume-regulated anion channels: evidence for colocalization with store-operated channels. *FASEB J*. 16:222–4.
48. Horne DJ, *et al*. (2012) Common polymorphisms in the PKP3-SIGIRR-TMEM16J gene region are associated with susceptibility to tuberculosis. *J. Infect. Dis*. 205:586–94.
49. Bowman AB, *et al*. (2007) Duplication of Atxn1l suppresses SCA1 neuropathology by decreasing incorporation of polyglutamine-expanded ataxin-1 into native complexes. *Nat. Genet*. 39:373–9.
50. Dehnert M, *et al*. (2012) Seropositivity of Lyme borreliosis and associated risk factors: a population-based study in Children and Adolescents in Germany (KiGGS). *PLoS ONE*. 7:e41321.
51. Pachner AR. (1988) Borrelia burgdorferi in the nervous system: the new "great imitator." *Ann. N. Y. Acad. Sci*. 539:56–64.
52. Bartha I, *et al*. (2013) A genome-to-genome analysis of associations between human genetic variation, HIV-1 sequence diversity and viral control. *Elife*. 2:e01123.
53. Liveris D, *et al*. (2011) Improving the yield of blood cultures from patients with early Lyme disease. *J. Clin. Microbiol*. 49:2166–8.

Cite this article as: Hammer C, *et al*. (2015) A coding variant of *ANO10*, affecting volume regulation of macrophages, is associated with *Borrelia* seropositivity. *Mol. Med*. 21:15–26.